Wind and Structures, *Vol. 19, No. 4 (2014) 443-465*
DOI: http://dx.doi.org/10.12989/was.2014.19.4.443

Aerodynamic and aero-elastic performances of super-large cooling towers

Lin Zhao[1a], Xu Chen[*1], Shitang Ke[2b] and Yaojun Ge[1c]

[1]*State Key Laboratory for Disaster Reduction in Civil Engineering, Tongji University, Siping Road 1239, Shanghai 200092, China*
[2]*Department of Civil Engineering, Nanjing University of Aeronautics and Astronautics, Youdao Road 29, Nanjing 210016, China*

(Received March 25, 2013, Revised August 20, 2014, Accepted September 1, 2014)

Abstract. Hyperbolic thin-shell cooling towers have complicated vibration modes, and are very sensitive to the effects of group towers and wind-induced vibrations. Traditional aero-elastic models of cooling towers are usually designed based on the method of stiffness simulation by continuous medium thin shell materials. However, the method has some shortages in actual engineering applications, so the so-called "equivalent beam-net design method" of aero-elastic models of cooling towers is proposed in the paper and an aero-elastic model with a proportion of 1: 200 based on the method above with integrated pressure measurements and vibration measurements has been designed and carried out in TJ-3 wind tunnel of Tongji university. According to the wind tunnel test, this paper discusses the impacts of self-excited force effect on the surface wind pressure of a large-scale cooling tower and the results show that the impact of self-excited force on the distribution characteristics of average surface wind pressure is very small, but the impact on the form of distribution and numerical value of fluctuating wind pressure is relatively large. Combing with the Complete Quadratic Combination method (hereafter referred to as CQC method), the paper further studies the numerical sizes and distribution characteristics of background components, resonant components, cross-term components and total fluctuating wind-induced vibration responses of some typical nodes which indicate that the resonance response is dominant in the fluctuating wind-induced vibration response and cross-term components are not negligible for wind-induced vibration responses of super-large cooling towers.

Keywords: cooling tower; aero-elastic model; self-excited force; wind-induced vibration response

1. Introduction

In recent years, there is an increasing need to enhance the capacity of power-plant structures such as large cooling towers to require power demand in developing countries (Babu *et al*. 2013). Large high-capacity cooling towers are increasingly becoming necessary in developed countries as

*Corresponding author, Ph.D. Student, E-mail: zui1988@126.com
[a] Associate Professor, E-mail: zhaolin@tongji.edu.cn
[b] Assistant Professor, E-mail: keshitang@163.com
[c] Professor, E-mail: yaojunge@tongji.edu.cn

http://www.techno-press.org/?journal=was&subpage=8 ISSN: 1226-6116 (Print), 1598-6225 (Online)

many towers are more than 30 years and required to be replaced. Due to the failure of cooling towers in Ferrybridge in England in 1965 (Bamu and Zingoni 2005), they have attracted attention of many researchers in the world and a lot of research work on the wind resistance of cooling towers has been reported in the literature mainly including wind load characteristics of cooling towers (Armitt 1980, Goudarzi *et al*. 2008, Borri *et al*. 2011), wind-induced response and equivalent static wind loads of cooling towers (Zahlten and Borri 1998, Murali *et al*. 2012, Ke *et al*. 2012), wind-induced interference effects on group cooling towers (Niemann and Köpper 1998, Orlando 2001), CFD simulation (Meroney 2008), wind-induced buckling analysis (Xu and Bai 2013).

In China, with the development of power industry, groups of super-large cooling towers arranged with a high density have been built in many parts, and the distances among towers and the heights of towers have exceeded the minimum requirements of tower heights and tower distances specified in the "Code for design of cooling for industrial recirculating water" (GB/T 50102-2003). The interferences for groups of cooling towers and the effects of wind-induced vibrations are very prominent which need a higher requirement for the wind resistance design of cooling towers, especially under the strong typhoon conditions (Zhao *et al*. 2013). In the 1970s, Isyumov (1972) and Armitt (1980) pointed out that dynamic stresses and static stresses of cooling towers under wind loads have the same order of magnitude based on wind tunnel tests of traditional cooling tower elastic models, and resonant stresses are increased by the fourth power of wind speed, which are much higher than the increment speed of quasi-static stresses and indicated that effect of wind-induced vibration responses of cooling towers cannot be ignored. The wind-induced vibration responses of cooling towers cannot be directly obtained by means of commonly used wind tunnel test methods such as synchronous surface pressure measurements and basal high-frequency balance force measurements. The method for calculating magnification factors of wind-induced vibration response forces of cooling towers based on the time history of surface aerodynamic force obtained by synchronous pressure tests also has the problems such as the self-excited aerodynamic force related to the movement form is difficult to be described and etc. Accordingly, the technology of wind tunnel test of cooling towers shall be developed further, the design and key processing links of aero-elastic models shall be improved, and the engineering practice shall be economically and reasonably guided by combining with the super-large development requirements of the current cooling tower engineering.

Fig. 1 Layout plan of the power plant

Table 1 Size characteristics of major components of the cooling tower (Unit: m)

Component	Ground clearance	Center radius	Thickness of tube wall	Concrete grade
Main structure	19.80	77.99	1.80	C30
	35.49	73.01	0.41	
	51.28	68.24	0.40	
	70.07	63.02	0.39	
	89.00	58.37	0.39	
	106.64	54.76	0.39	
	128.88	51.41	0.37	
	148.31	49.81	0.33	
	166.31	49.55	0.27	
	190.29	50.43	0.27	
	206.77	51.20	0.26	
	214.26	51.56	0.45	
Suport structure	48 pairs of herringbone columns with a diameter of 1.30m			C40

The background of this paper is based upon a nuclear power plant project which adopts four high catchment natural draft cooling towers (see Fig. 1). The height of each tower is 215 m, the height of the throat part is 160 m, the diameter of the point with a height of zero meter is 169.48 m, and the area of spraying is 18300 m^2. Moreover, the towers are researched and designed by the State Nuclear Electric Power Planning Design & Research Institute and Harmon of Belgium, the research for the wind tunnel test, wind-induced response and equivalent static wind loads of the project is charged by Tongji University, and the height and spraying area of the tower completed will be the largest in the world. More information about size characteristic of major components of cooling towers can be referred from Table 1.

2. Traditional continuous medium aero-elastic model

Hyperbolic cooling towers belong to typical thin shell structures (the minimum wall thickness is about 250 mm), which have complicated vibration modes and are sensitive to wind load effects. Due to the design and processing difficulty, cooling tower aero-elastic models actually used at home and abroad have shortages in the likelihood ratio simulations of physical parameters and aerodynamic parameters and etc., and therefore the applications for the results of wind tunnel test on the projects are limited to some extent. The design of such aero-elastic models has the following characteristics: a) adopt a model design with a large scale ratio (about 1: 600); b) simulate the scale stiffness and geometric shape by means of an isotropic and continuous medium thin shell material; c) give up the simulation of Froude number, the wind speed ratio of wind tunnel test is about 1: 3, and the structure frequency ratio is about 200: 1; d) lack of verification and modification methods for the effect of the Reynolds number and Strouhal number of surface circumferential motion of cooling tower models; e) the measuring equipments of wind-induced vibration response shall be contact strain gauges, acceleration sensors, non-contact laser displacement meters and etc.

The design characteristics above will lead to the effects as follows:

(1) Under the condition of designed wind speeds of prototype cooling towers, the general wind-induced vibration displacement of the shell is 100 mm to 200 mm, the range of wind-induced vibration displacement of a large scale ratio is between 0.17 mm and 0.34 mm, compared with the measurement accuracy of the minimum dynamic displacement of a laser displacement meter which is about 0.05 mm, the test error can reach 15% to 30%. If the laser displacement meter and the bracket are arranged upstream the cooling tower, the impact of the laser displacement meter as an interference object cannot be ignored and if other contact measurement methods are applied, the impacts for the stiffness and weight of the sensor on the dynamic characteristics of thin-walled models also cannot be ignored.

(2) In the scale stiffness simulation process of cooling tower aero-elastic models, the axial stiffness and bending and torsion stiffness of thin-walled components have two to three orders of magnitude in the design difference. Generally, there is no an ideal material meeting the scale requirements of elastic modulus and shear modulus, and the scale requirements for the two kinds of stiffness above cannot be simultaneously met just by regulating the thickness of a single wall when the scale stiffness is simulated with an isotropic and continuous medium thin shell material. The results of approximate simulation will inevitably cause the mismatching of the model dynamic characteristics and the design requirements. In allusion to the size and wind resistance rate requirements for the wind tunnel test section of the various domestic and foreign boundary layers, the reasonable scale ratio of the available cooling tower is about 1: 600 to 1: 200, the stiffness component of traditional aero-elastic model is an epoxy material, and the elasticity modulus is about 1/10 of concrete. In Table 2, the stiffness simulation of an aero-elastic model with different scale ratios is compared, in which the conversion relationship of likelihood ratio of simulated Froude number is considered, and the scale ratio requirement of the bending and torsion stiffness is preferentially met in the scale of wall thickness. According to the comparison, it can be indicated that the scale ratio requirement cannot be simultaneously met by the axial stiffness and bending and torsion stiffness, and the ratio for the simulated value of axial stiffness to the designed value is between 4.47 and 7.74 under the premise that the bending and torsion stiffness is in line with the scale ratio requirement.

(3) When the simulation of Froude number is considered for giving up, the design frequency ratio between the model and the prototype structure is 200: 1, the frequency (about 100 to 200 Hz) of the model is far excessive to the effective frequency range of fluctuating wind which can be simulated in the wind tunnel, and the problem of high frequency interference is obvious.

(4) The aerodynamic parameters related to the model scale ratio directly affect the stress state of the structure. For the prototype structure of cooling tower, the Reynolds number is about 10^8, the surface circumferential motion is in a post-critical state, the Reynolds number of the reduced-scale model is about 5×10^5, the surface circumferential motion is in a supper-critical state, the prototype structure of cooling tower and the reduced-scale model are significantly different in the position of surface circumferential motion separation point, the minimum negative pressure area and the pressure value of back flow area. The resistance coefficient of the overall structure and the Strouhal number related to the vortex-induced force are also affected by the Reynolds

number. As the differences between the Reynolds numbers of the reduced-scale model and the prototype structure may lead to static and dynamic force responses of the structure to cause essential difference, the effect simulation of the aerodynamic parameters shall be carried out seriously.

3. Equivalent beam-net aero-elastic model

In section2, it can be seen clearly that traditional continuous medium aero-elastic models have some shortages in the design and test methods of models. In allusion to these shortages, the so-called “equivalent beam-net design method” of aero-elastic model of cooling towers is proposed. The main idea of this method is that the approximate simulation for the structural dynamic characteristics of continuous shell is carried out by means of a spatial vertical and horizontal cross-truss mesh structure. For the model local position, both the thickness and width of orthogonal truss unit can be regulated optionally, so that the two types of stiffness scale relationship of a multi-parameter regulable aero-elastic model can be realized, and the problem of inconsistent stiffness can be avoided. Main design of this method is as follows:

Step.1: finely modeling the shell element of tower drum of the cooling tower in order to obtain dynamic characteristics of the structure. The modeling of cooling tower structure is carried out by means of a finite element method, wherein the tower drum is discretized as spatial shell elements, the stiffening rings on the top of the tower and the 48 pairs of herringbone columns connected to the ring base are simulated by means of spatial beam elements, and the bottom of the herringbone columns is fixedly connected.

Table 2 Stiffness simulation comparison of aero-elastic model of different scale ratios

<table>
<tr><th rowspan="2">Parameter</th><th rowspan="2">Requirements of likelihood ratio</th><th colspan="2">Scale ratio λ_L = 1: 600</th><th colspan="2">Scale ratio λ_L = 1: 200</th></tr>
<tr><th>Designed value</th><th>Simulated value</th><th>Designed value</th><th>Simulated value</th></tr>
<tr><td>Modular ratio</td><td>λ_E , λ_G</td><td>1:600</td><td>1:10</td><td>1:200</td><td>1:10</td></tr>
<tr><td>Wall thickness scale ratio</td><td>λ_D</td><td>1:600</td><td>1:1670</td><td>1:200</td><td>1:423</td></tr>
<tr><td>Bending stiffness ratio</td><td>$\lambda_{EI} = \lambda_E \times \lambda_L^4$</td><td colspan="2" rowspan="2">1:7.78×10^{13}</td><td colspan="2" rowspan="2">1:3.20×10^{11}</td></tr>
<tr><td>Torsion stiffness ratio</td><td>$\lambda_{GJ} = \lambda_G \times \lambda_L^4$</td></tr>
<tr><td>Axial stiffness ratio</td><td>$\lambda_{EA} = \lambda_E \times \lambda_L^2$</td><td>1:2.16×$10^8$</td><td>1:2.79×$10^7$</td><td>1:8.00×$10^6$</td><td>1:1.79×$10^6$</td></tr>
<tr><td colspan="2">λ_{EA} designed value/λ_{EA} simulated value</td><td colspan="2">1:7.74</td><td colspan="2">1:4.47</td></tr>
</table>

Step.2: modeling spatial beam elements, wherein the number of meridian beam element is m, the number of circular beam element is n, the number of the maximum regulable unit is $2(2\ m+1)n$; with the consideration for the circular symmetry of the cooling tower structure, simplifying the meridian thickness and width variable to $D_{ver\cdot i}$, $W_{ver\cdot i}$, i = 1, m, simplifying the circular thickness and width variable to $D_{cir\cdot j}$, $W_{cir\cdot j}$, j = 1, m+1, and reducing the number of the variable to $4\ m+2$ (see Fig. 2).

Step.3: with the consideration for the convenient processing performance of the model, using continuous components with equal thickness as the meridian beam element, simplifying $D_{ver\cdot i}$ to a single variable X_0, and then calculating the constant matrix $\{C_{bending.\ i}\}$, $\{C_{axial.\ i}\}$, i = 1, m for the anti-bending and axial scale stiffness of the drum of different height unit sizes. Assuming that the size and scale stiffness of model component of the cooling tower are in line with the linear combination conditions

$$\begin{aligned} &\{D_{ver.i}\} = X_0\{E\}_{1\times m} \\ &\begin{bmatrix} \{W_{ver.i}\} \\ \{D_{cir.i}\} \\ \{W_{cir.i}\} \end{bmatrix} = \kappa \times \left[\{C_{bending.i}\} \quad \{C_{axial.i}\}\right] \times \begin{bmatrix} X_1 & X_3 & X_5 \\ X_2 & X_4 & X_6 \end{bmatrix} \end{aligned} \tag{1}$$

By considering a large number of vertical and horizontal connection nodes $(m+1)n$ in the model assembly process are connected by welding and the cumulative effect of stiffness loss in the node point is large, a stiffness commutation factor κ is introduced in Eq. (1). During the model design process, it is necessary to create a stiffness loss relationship through the measured dynamic characteristic values of pre-processed model, and the corresponding stiffness modification methods shall be taken therein. In Eq. (1), the number of the variable is further simplified to 6 to 7. Generally, the modes for the front 6 to 8 orders can be taken as simulation objectives on the basis of modeling dynamic characteristic results of shell element of the cooling tower, in which the initial values X_1 to X_6 are provided, the values are in iterative calculation, the variable value is regulated, and a better simulation effect can be obtained generally.

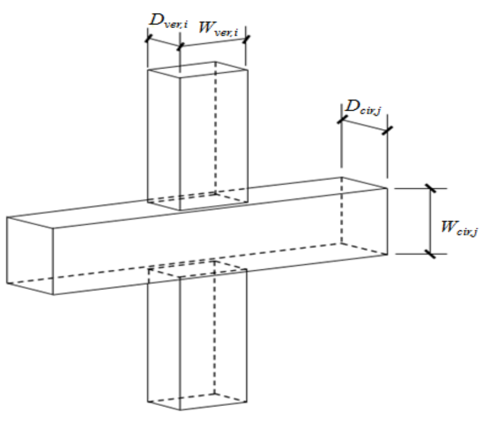

Fig. 2 Detailed figures and geometrical sizes of spatial beam elements

Table 3 Structural dimensions and additional masses of the equivalent beam-net aero-elastic model

Structural members	Ground clearance (mm)	Centre radius (mm)	Circular size (mm)		Meridian size (mm)		Additional mass (g)
			Thickness	Width	Width	Thickness	Mass × 36
Shell	170.27	367.29	0.80	10.00	12.00	0.80	90×36
	242.02	345.44	0.80	10.00	10.00	0.80	25×36
	314.13	324.84	0.80	7.00	10.00	0.60	23×36
	386.66	305.77	0.80	7.00	8.00	0.60	21×36
	459.67	288.60	0.80	7.00	6.00	0.60	20×36
	533.18	273.78	0.60	5.00	6.00	0.40	19×36
	607.21	261.81	0.60	5.00	6.00	0.40	18×36
	681.71	253.20	0.60	5.00	6.00	0.40	17×36
	756.55	248.42	0.60	5.00	6.00	0.40	15×36
	831.54	247.73	0.60	5.00	6.00	0.40	12×36
	831.54	247.73	0.60	5.00	6.00	0.40	12×36
	906.50	250.17	0.60	5.00	8.00	0.60	12×36
	981.42	253.52	0.80	5.00	8.00	0.60	30×36
	1069.50	260.03	1.00	5.00			
Stiffening ring	1069.50	260.03	Wire with a radius of 0.5 mm and a round cross section				
Top of herringbone column	99.00	415.00	Wire with a radius of 2.0 mm and a round cross section				

The material components of beam elements of the aero-elastic model can be thin galvanized sheet steels, the increment for the thickness of standard profile is 0.1 mm, the thickness is between 0.1 to 1.0 mm, the width direction is processed by means of a linear cutting method, and the accuracy of size processing is 0.01 mm.

According to the requirements of geometric likelihood ratio, the appearance of an actual cooling tower is simulated by pasting a whole elastic and lightweight membrane with a tension performance on the outer surface of the steel frame, wherein the coat is basically prevented from stiffness supply and surface gaps, and the coat which is tensioned will not have obvious local wind-induced vibration and deformation under the effect of wind speed and provide an excessive damping ratio as well (see Fig. 3(a)).

For the equivalent beam-net model, the quality simulation is an important part. According to the requirements for the likelihood ratio of the cooling tower quality system, the actual mass of the steel frame shall be deducted, and the mass of the short part can be supplemented by using *(m+1)n* groups of copper lead blocks as balance weights. In this paper, a "removable" quality system is developed, specifically each node is equipped with a connection pipe, of which the interior is applied to the arrangement of pressure measuring pipe, so that the wind tunnel test for synchronously measuring pressures and vibrations of the aero-elastic model can be implemented and the outer edge is used for fixing the “attachable” quality system, quality system is firmly fixed without providing too much damping and convenient in assembling (see Fig. 3(b)). When the quality system is removed, the basic frequency of the model structure is about 30 to 40Hz, the model is approximated as a rigid model, and therefore the pressure measuring test of "rigid” and aero-elastic model can be carried out in allusion to the same cooling tower model, and the impacts of self-excited force effect on the surface wind pressure and wind-induced response of the cooling tower can be researched.

As the shear capacity of the aero-elastic model in the vertical and horizontal nodes is relatively weak and each small element is an unstable quadrangle composed of several geometries, the aero-elastic model has a pulse wind pressure impact on the local shell under the excitation of wind load. In response to the problem, each node is further provided with a thin round piece with a diameter of 40 mm and a thickness of 0.5 mm to increase the anti-shear capacity of the node and increase the stability of the local quadrilateral element under the excitation of wind load (see Fig. 3(b)). Fig. 3(c) shows the comparison for the overall dynamic characteristics of the structure before and after taking the proposal, and indicates that the improvement effectiveness for the overall frequency of the structure after increasing the thin round piece is obvious.

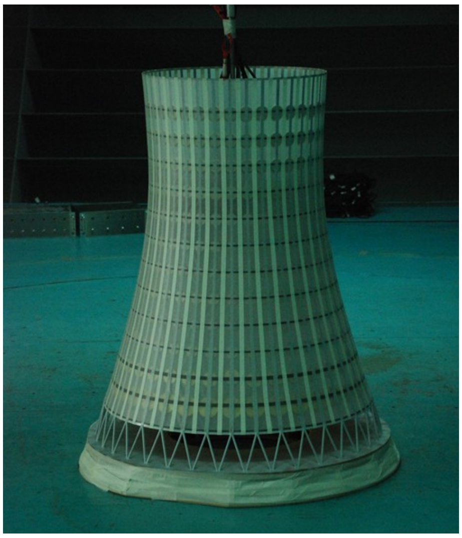

(a) Aero-elastic model with thin plastic membrane

(b) Arrangement of the quality system with thin round pieces

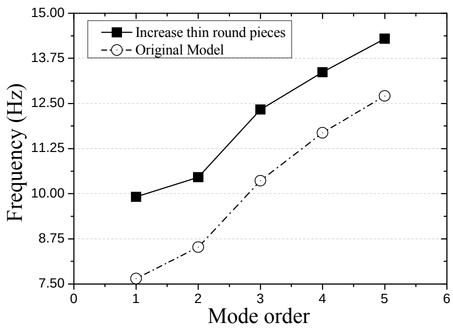

(c) Change of dynamic characteristics after increasing anti-shear components

Fig. 3 Aero-elastic model with the quality system and thin round pieces

Table 4 Debugging results for dynamic characteristics of beam-net aero-elastic model

Order	Modeling of shell element			Modeling of beam-net		Model measurement
	Mode	Vibration mode description	Prototype frequency (Hz) / Model frequency (Hz)	Mode	Designed frequency (Hz) / Designed error (%)	Measured frequency (Hz) / Measured error (%)
1,2	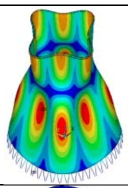	four circular harmonic waves Two vertical harmonic waves	0.660	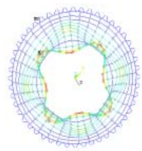	9.91	9.71
			9.90		0.01	-2.00
3,4	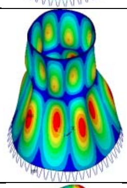	Five circular harmonic waves Two vertical harmonic waves	0.690	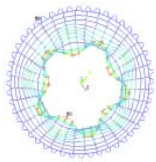	10.45	11.48
			10.35		0.1	9.87
5,6	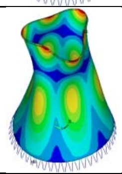	Three circular harmonic waves Two vertical harmonic waves	0.820	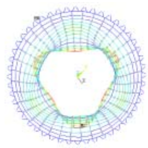	12.33	13.43
			12.30		0.01	8.95
7,8	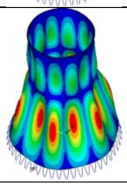	Six circular harmonic waves Two vertical harmonic wave	0.891	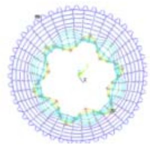	13.36	14.62
			12.60		5.60	8.61

The great advantage of the equivalent beam-net method is that the stiffness of the vertical and horizontal beam can be optionally regulated to solve the problem for the inconsistent scale ratio between the axial stiffness and the bending and torsion stiffness of the shell. Generally, the aero-elastic model designed by means of an equivalent beam-net method can obtain better results during the dynamic characteristics test process, and the frequencies for the front eight orders of the structure can be simulated. Table 3 gives the structural dimensions and additional masses of the equivalent beam-net aero-elastic model of the 215 m cooling tower. The beam-net model above is subjected to a dynamic characteristic test to inspect whether the dynamic characteristics of the aero-elastic model are in line with the requirements of wind tunnel test. As the low-level frequencies of the model are more sensitive to the wind load effect, the modes of several front orders are mainly simulated during the debugging process. The frequency for the front eight orders of the model is obtained by means of the initial displacement excitation of the model and the time sequence of the low wind speed turbulent buffeting response, and the model vibration mode is temporarily unable as the vibration mode of the cooling tower is very complicated. The simulated debugging results are shown in Table 4. For the measured frequency, the relative error can be controlled within about 10%. The mode damping ratio of the first order is 3.5%, which is basically in line with the requirements of the specifications for concrete structural damping ratio.

4. The introduction of wind tunnel test

The test is carried out in the wind tunnel of TJ-3 atmospheric boundary layer in the State Key Laboratory of Disaster Reduction in Civil Engineering, Tongji University. The wind tunnel is a closed reflux rectangular cross-section wind tunnel, wherein the size of the test section is as follows: the width is 15 m, the height is 2 m, and the length is 14 m. In the test, the air flow of the atmospheric boundary layer is considered as the landform of Class B, the wind speed change index along the height is 0.15, and the near-earth turbulence intensity is 20%. During the simulation process of atmospheric boundary layer within the wind tunnel, the similarity for the parameters of the following three aspects shall be considered: wind profile, turbulence intensity profile and fluctuation wind speed spectrum. After debugging, the wind field of atmospheric boundary layer in the landform of Class B with the scale ratio of 1: 200 is simulated by means of a passive turbulence generating device with combined spires and roughness elements (see Fig. 4). Fig. 5 shows the measured average wind profile, turbulence intensity and fluctuating wind speed spectrum of the flow field of Class B, and indicates that the average wind profile simulated in the wind field is relatively in line with the regulation, the turbulence intensity in the point near the surface is about 15%, which is also in line with the relevant regulation. The measured fluctuating wind speed spectrum is fitted and compared with the curves of Davenport spectrum, Harris spectrum and Karman spectrum, in which it can be found that the wind tunnel measured spectrum is relatively close to the Karman spectrum. The congestion indexes of the cooling tower and the surrounding building models are less than 5%.

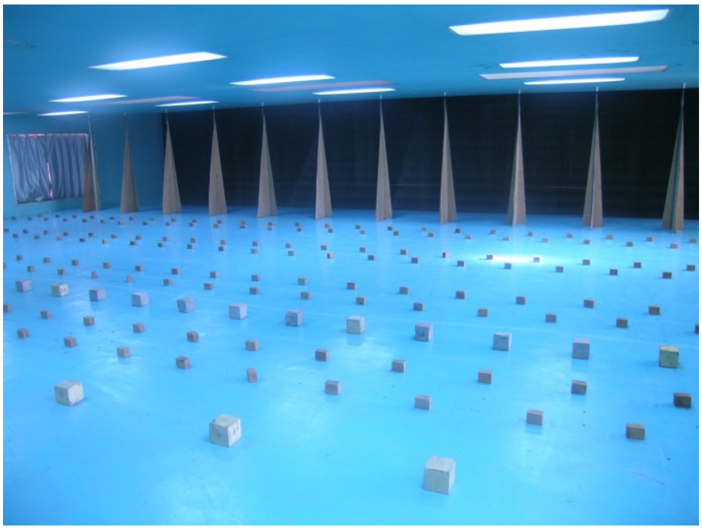

Fig. 4 Simulation device for wind field of Class B of atmospheric boundary layer

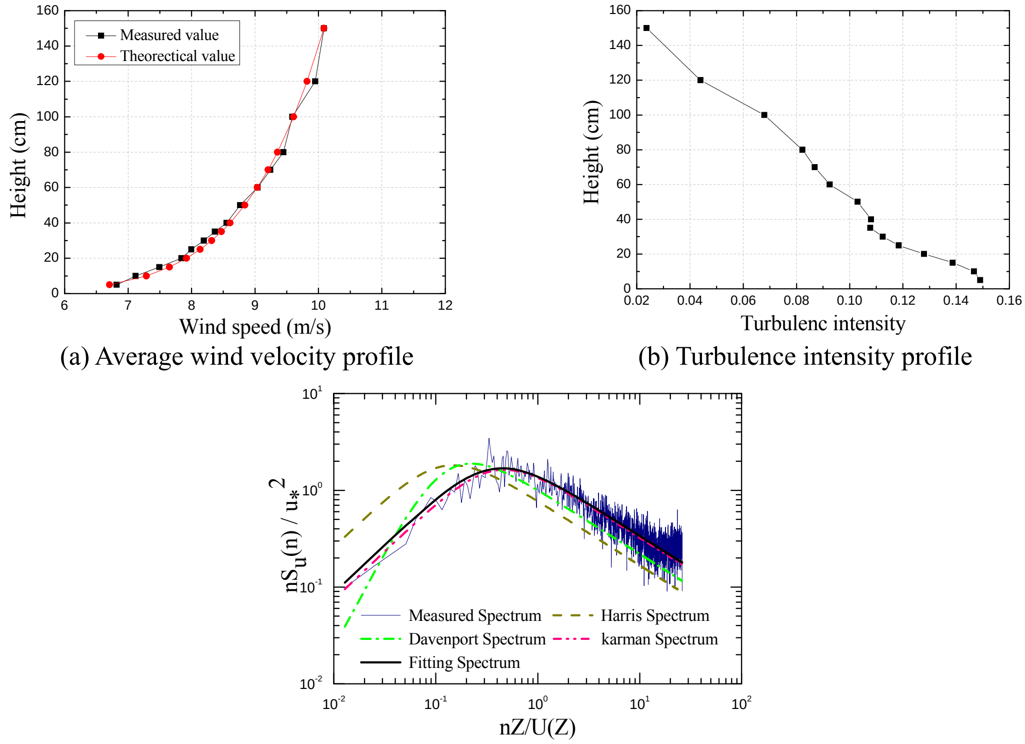

(a) Average wind velocity profile

(b) Turbulence intensity profile

(c) Power spectrum density along wind component

Fig. 5 Wind environment parameters of Type B terrain in TJ-3 wind tunnel

The equivalent beam-net aero-elastic model firstly proposed by Zhao and Ge (2010) is adopted, and aerodynamic pressures around the surface of the cooling tower and wind-induced responses are measured synchronously. The pressure measuring points of the cooling tower are arranged in the crossing point positions of vertical and horizontal beams, 12 sections are totally arranged along the meridian direction and 36 pressure measuring points are evenly arranged along the circular direction by considering the obvious three-dimensional space effect of the wind inlet and outlet sections. 8 displacement measuring points are evenly arranged along the circular direction while measuring the vibration, and 6 different measuring heights are arranged along meridian direction (see Fig. 6). During the test process of vibration measurement of aero-elastic model, a variety of measuring point along the circumferential direction of the same height of the cooling tower are synchronously measured, and the displacement measurement at different heights is conducted by regulating the position for the tray of laser displacement meter.

The debugging and measurement for the simulated wind field of the atmospheric boundary layer are carried out by means of Streamline hot-wire anemometer of DANTEC Company of Denmark. The measurement for the average pressure of internal and external surfaces of the cooling tower and the measurement of fluctuating pressure are carried out by means of the DSM3000 electronic pressure scanning valve of Scanivalve of the United States. The signal sampling frequency is 312.5 Hz, the total length for the sample sampled from each measuring point is 6000 data. The displacement response measurement and analysis system of the model is composed of a non-contact LM10 type laser displacement sensor produced by Panasonic Company of Japan, a 5.18 cassette collection instrument produced by Dongfang Vibration and Noise Institute of Technology, and a DASP2000 Professional signal analysis system. The signal sampling frequency of wind-induced vibration is 200 Hz, and sampling time is 30 seconds. In addition, a HP35670 which is a type dynamic signal analyzer produced by Hewlett-Packard Company of the United States is also used to monitor the test signal in real time in the test process.

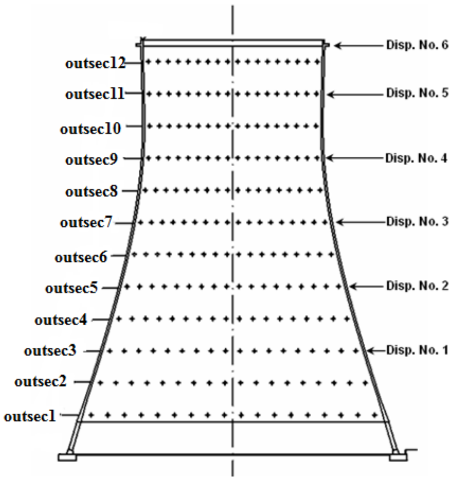

(a) Taps for external pressure (on left) and wind-induced displacement (on right)

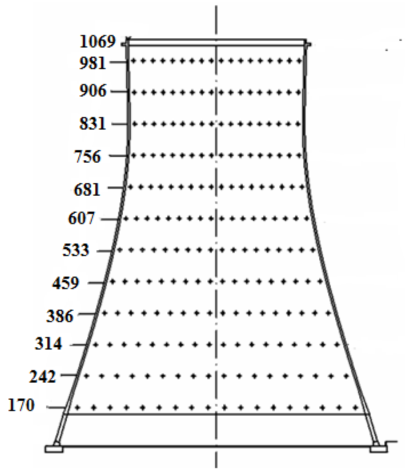

(b) Height of taps (unit: mm)

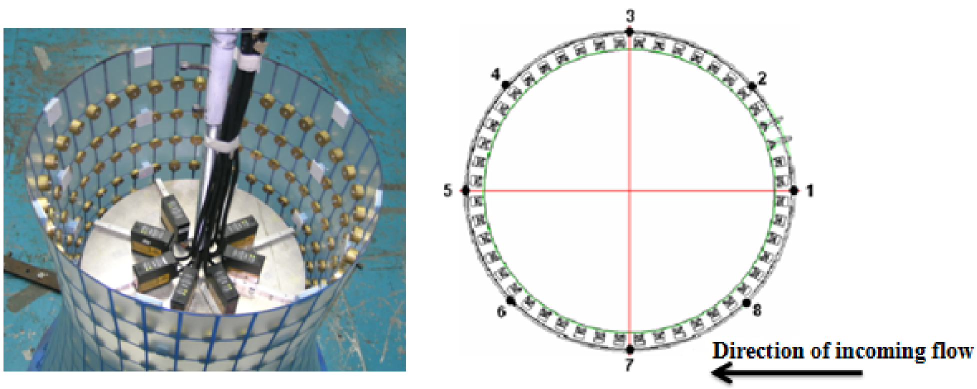

(c) Arrangement of displacement sensors along the circumferential direction

Fig. 6 Measuring point arrangement for surface pneumatic pressure and wind-induced displacement response of the aero-elastic model

5. Simulation of effects of Reynolds number and Strouhal number

For the conventional wind tunnel test of a model with a large scale ratio (1: 200 to 1: 500) of hyperbolic cooling tower with a circular section, the impact of the Reynolds number effect on the circumferential motion form of external surface is very prominent. In this paper, the Reynolds number range of the prototype structure of large cooling tower under the designed wind speed is from 3.5×10^8 to 5.5×10^8, while in the wind tunnel test, the number fluctuates from 2.0×10^5 to 4.0×10^5 which is 2 ~ 3 orders of magnitude smaller than the prototype structure under the design speed. Due to the local limitation of physical wind tunnel, the surface circumferential motion form under such a high Reynolds number is difficult to be represented by means of a simple method of improving test wind speed or increasing the geometric size of the structure model. As experience proves that the circumferential motion characteristics under a high Reynolds number can be approximately simulated by properly changing the surface roughness of the model and modifying testing wind speeds, and a lot of research information is available (Simiu and Scanlan 1996, Zhao and Ge 2010).

This paper selects 36 pressure taps in the throat part (the section of outsec10 in Fig. 6(a)) and measures the distribution for the wind pressure shape coefficients of model surface of a full aero-elastic model and a "rigid model" without the quality system in the turbulence flow flied of Class B under the condition of different test wind speeds (6 m/s to 12 m/s) and different surface roughness. The surface roughness is simulated with the aid of sticking paper taps along the meridian direction, wherein the width of each paper tap is 10 mm, and the thickness is 0.1 mm. The simulation standard is the eight items of wind pressure distribution curve in the Chinese code (GB/T 50102-2003 and DL/T 5339-2006) and the mean surface pressure of ribless hyperbolic cooling towers under post-critical Reynolds are suggested as follows

$$u_p(\theta) = \sum_{k=0}^{7} a_k \cos k\theta \tag{2}$$

in which θ is the angle ($0 \le \theta \le \pi$), a_k is the fitting parameter (a_0=-0.4426, a_1=0.2451, a_2=0.6752, a_3=0.5356, a_4=0.0615, a_5=-0.1384, a_6=0.0014, a_7=0.0650).

The simulation process focuses on the comparison of the maximum pressure coefficient of surface circumferential motion, the minimum pressure coefficient, the wake flow pressure coefficient, the angle of zero pressure coefficient, the angle of the minimum pressure coefficient, and separation angle. In the code, it suggests that the maximum pressure coefficient and its angle is 1.0 and 0^o, respectively, the minimum pressure coefficient and its angle is -1.627 and $\pm 70^o$, respectively, zero pressure angle is $\pm 33^o$, separation angle is $\pm 120^o$, average pressure coefficient of wake flow is about -0.4. By trying to stick paper tapes of different layers and regulate different wind speeds of incoming flow on the “rigid model”, the simulation proposal of Reynolds number effect chooses the even attachment of three layers of paper tapes along the meridian direction combined with the incoming flow wind speed of 8 m/s. Fig. 8(a) shows the comparison among standardized curve and the wind pressure shape coefficients with different surface roughness in the incoming flow wind speed of 8 m/s. Fig. 8(b) shows the comparison between the “rigid model” and the aero-elastic model.

According to the comparison between the surface wind pressure distribution characteristics of the aero-elastic model and rigid model under the same Reynolds number simulation method (see Fig. 7(b)), it can be found that the biggest difference for the surface circumferential motion characteristics of the aero-elastic model is that the minimum pressure coefficient angle is increased by 10°, and the negative pressure value of the protected area is slightly reduced. However, the overall wind pressure coefficient curve is consistent, there is no essential difference, and so that it can be indicated that the impact of self-excited force effect of large cooling tower on the average surface wind pressure is very small. Fig. 7(c)) provides the root variance distribution curve of shape coefficient under two working conditions, which shows that the symmetry of the root variance distribution excluding the self-excited force is relatively good, and the symmetry is completely broken when the fluctuating wind pressure includes the self-excited force effect, moreover, compared with most part of the rigid model pressure measurement, the numerical value of root variance is relatively large while considering the self-excited force. So far, there is no measured data for the extreme value distribution of surface wind pressure coefficient of large cooling tower, the deep comparison between the surface wind pressure coefficients of the rigid model and aero-elastic model cannot be carried out.

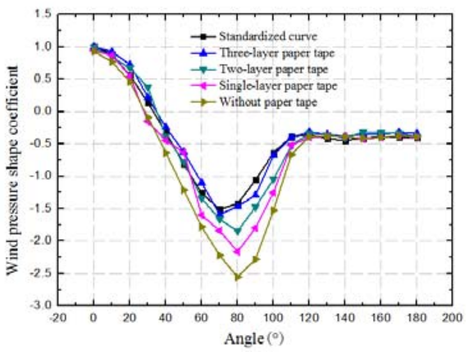

(a) Standardized curve and the wind pressure shape coefficients of different surface roughness with wind speed of 8 m/s

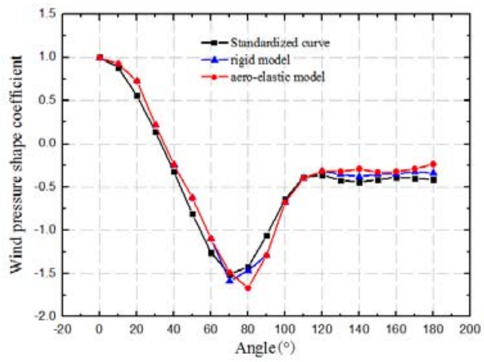

(b) Wind pressure shape coefficients of the "rigid model" and aero-elastic model

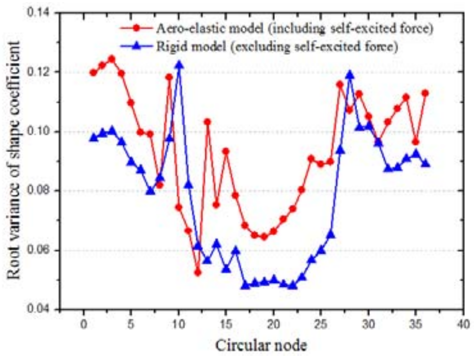

(c) Root variance distribution of circular surface shape coefficient

Fig. 7 Distribution curve for surface wind pressure characteristics of cooling tower

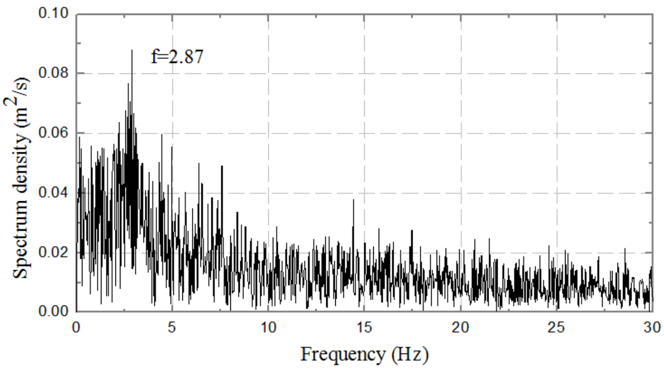

Fig. 8 The vortex shedding frequencies of the wake flow

Strouhal number is a function of structure geometry and Reynolds number. When the Reynolds number is more than 3.5×10^6, the turbulence composition in the wake flow vortex shedding of the cylindrical structure is more prominent, but the regular vortex shedding also will be presented, and the Strouhal number is slightly larger than 0.2 (about 0.22 in the Chinese code "GB/T 50102-2003" and "DL/T 5339-2006"). Strouhal number is closely related to the structural dynamic response, and is also one of the Reynolds number effects to be simulated in the test. Due to the irregularity of wake flow fluctuation composition, the operation for directly measuring the vortex shedding frequency is more difficult, so the paper attempts to indirectly determine the outstanding frequency of vortex shedding through the frequency spectrum function for the time interval of across-wind aerodynamic integral of the pressure measuring test, and simultaneously measure a variety of points in the wake flow by means of the hot-wire anemometer (see Fig. 8). It can be found from the figure that the vortex shedding frequency of the wake flow is 2.87Hz and the corresponding Strouhal number is 0.215 (in which the throat diameter of the cooling tower model is 0.60 m, and the wind speed is 8 m/s), which is more than 0.2 and further validates that the scale model of the cooling tower is fully in line with the target value requirements of the test.

6. Analysis of wind-induced vibration coupling effect

From the structural dynamic equations, the paper firstly derives the covariance matrix of displacement response of generalized resonance modal, subsequently obtains the covariance matrix of an elastic restoring force only including resonance components on the basis of IWL theory, and lastly carries out resonance response and calculation of equivalent static wind load by means of the load-response correlation (LRC method) method (Kasperski and Niemann 1992). The method can more fully consider the calculation of the resonant mode coupling effects, and overcome the shortages of traditional inertia wind load method (IWL method) (Zhang 2002) and gust load factor method (GLF method) (Davenport 1967) in the analysis accuracy of processing the resonant component coupling of each order to some extent.

6.1 Covariance matrix of generalized resonant modal response

The response of the structure to the stochastic wind excitation can be described as the following equation

$$[M]\{\ddot{y}\}+[C]\{\dot{y}\}+[K]\{y\}=[R]\{p(t)\} \tag{3}$$

in which $[M]$, $[C]$ and $[K]$ mean mass, damping and stiffness matrix, respectively; $\{\ddot{y}\}$, $\{\dot{y}\}$ and $\{y\}$ mean the joint acceleration, velocity and displacement vectors, respectively; $[R]$ is an power indicator matrix; $\{p(t)\}$ is an external wind excitation vector.

The response can be expanded as follows by means of a complete vibration mode

$$\{y(t)\}=[\Phi]\{q(t)\}=\sum_{i=1}^{n}\phi_i q_i(t)=\sum_{i=1}^{m}\phi_i q_i(t)+\sum_{i=m+1}^{n}\phi_i q_i(t)=\{y\}_d+\{y\}_s \tag{4}$$

in which $[\Phi]$ is the matrix of structural vibration modes; ϕ_i is the i-order vibration mode; q_i is the i-order generalized displacement vector; m is the number of mode only considering resonant component; n is the number of full modes; $\{y\}_d$ is a vibration response vector considering the front m-order resonant modes; $\{y\}_s$ is a vibration response vector only considering the rest quasi-static contribution of full modes.

The static response of the structure under the $\{p(t)\}$ load effect is $[K]^{-1}\{p(t)\}$, which also can be represented by the full vibration mode of the following formula

$$[K]^{-1}\{p(t)\}=\sum_{i=1}^{n}[I]_i\{p(t)\}=\sum_{i=1}^{m}[I]_i\{p(t)\}+\sum_{i=m+1}^{n}[I]_i\{p(t)\} \tag{5}$$

in which $[I]_i$ is the flexibility matrix of the i-order vibration mode. $\{y\}_s$ can be expressed as

$$\{y\}_s=\sum_{i=m+1}^{n}[I]_i\{p(t)\}=[K]^{-1}\{p(t)\}-\sum_{i=1}^{m}[I]_i\{p(t)\} \tag{6}$$

By combining with the Eq. (4), $\{y(t)\}$ can be expressed as the following formula

$$\begin{aligned}\{y(t)\}&=\{y\}_d+\{y\}_s=\sum_{i=1}^{m}\phi_i q_i(t)+[K]^{-1}\{p(t)\}-\sum_{i=1}^{m}[I]_i\{p(t)\}\\&=\sum_{i=1}^{m}(\phi_i q_i(t)-[I]_i\{p(t)\})+[K]^{-1}\{p(t)\}\end{aligned} \tag{7}$$

Thus the resonant response can be defined as

$$\{y(t)\}_r=\sum_{i=1}^{m}(\phi_i q_i(t)-[I]_i\{p(t)\}) \tag{8}$$

By combining with the Eq. (8), the i-order generalized modal response only including resonance components can be derived as

$$q_{r,i}(t) = q_i(t) - \frac{\phi_i^T \{p(t)\}}{\phi_i^T [K] \phi_i} = q_i(t) - \frac{F_i(t)}{K_i} \tag{9}$$

in which $F_i(t)$ is the *i*-order generalized external stochastic wind excitation; K_i is the *i*-order generalized stiffness.

Accordingly, the cross-power spectrum of the generalized resonant modal responses between *i*-order and *j*-order can be expressed as

$$\begin{aligned}
S_{q_{r,i},q_{r,j}}(\omega) &= \int_{-\infty}^{\infty} R_{q_{r,i},q_{r,j}}(\tau) e^{-i2\pi\omega\tau} d\tau = \int_{-\infty}^{\infty} E[q_{r,i}(t), q_{r,j}(t+\tau)] e^{-i2\pi\omega\tau} d\tau \\
&= \int_{-\infty}^{\infty} E[(\int_{-\infty}^{\infty} h_i(u) f_i(t-u) du - \frac{f_i(t)}{k_i})(\int_{-\infty}^{\infty} h_j(v) f_j(t+\tau-v) dv - \frac{f_j(t+\tau)}{k_j})] e^{-i2\pi\omega\tau} d\tau \\
&= \int_{-\infty}^{\infty} h_i(u) e^{-i2\pi\omega\mu} d\mu \int_{-\infty}^{\infty} R(\tau+u-v) e^{-i2\pi\omega(\tau+u-v)} d(\tau+u-v) \int_{-\infty}^{\infty} h_j(v) e^{-i2\pi\omega v} dv \\
&\quad - \frac{1}{k_i} \int_{-\infty}^{\infty} h_j(v) e^{-i2\pi\omega v} dv \int_{-\infty}^{\infty} R(\tau-v) e^{-i2\pi\omega(\tau-v)} d(\tau-v) \\
&\quad - \frac{1}{k_j} \int_{-\infty}^{\infty} h_i(u) e^{-i2\pi\omega u} du \int_{-\infty}^{\infty} R(\tau+u) e^{-i2\pi\omega(\tau+u)} d(\tau+u) + \frac{1}{k_i k_j} \int_{-\infty}^{\infty} R(\tau) e^{-i2\pi\omega\tau} d\tau \\
&= (H_i^*(\omega) H_j(\omega) - \frac{1}{K_i} H_j(\omega) - \frac{1}{K_j} H_i(\omega) + \frac{1}{K_i K_j}) S_{F_i,F_j}(\omega) \\
&= (H_i^*(\omega) - \frac{1}{K_i})(H_j(\omega) - \frac{1}{K_j}) S_{F_i,F_j}(\omega) = \dot{H}_i^*(\omega) \dot{H}_j(\omega) S_{F_i,F_j}(\omega)
\end{aligned} \tag{10}$$

in which $H_i(\omega)$ is the transfer function of the *i*-order mode; $\dot{H}_i(\omega) = H_i(\omega) - \frac{1}{K_i}$ is defined as the resonant transfer function of the *i*-order mode; $S_{F_i,F_j}(\omega)$ is the cross-power spectrum of the generalized external stochastic wind excitation.

According to all equations above, the covariance matrix of generalized resonant modal response $[C_{qq}]_r$ can be expressed as

$$[C_{qq}]_r = \int_{-\infty}^{\infty} \dot{H}^* S_{FF} \dot{H} d\omega = \int_{-\infty}^{\infty} \dot{H}^* \Phi^T R D S_{AA} D^T R^T \Phi \dot{H} d\omega \tag{11}$$

in which A, D are the time coordinate vector and intrinsic mode matrix by implementing POD decomposition (Tamura *et al.* 1999, Li *et al.* 2009). S_{AA} is the cross-power spectrum of time coordinate vector A.

6.2 Covariance matrix of elastic restoring force (only including resonance components)

According to the application of modal expansion theory, the elastic restoring force $\{P_{eqq}\}_r$ only including resonant components can be expressed as

$$\left\{P_{eqq}\right\}_r = [K][\Phi]\{q(t)\}_r = [M][\Phi][\Lambda]\{q(t)\}_r \tag{12}$$

in which $\{q(t)\}_r$ is the vector of generalized response only including resonant components; $[\Lambda] = diag(\omega_1^2, \cdots \omega_n^2)$, ω_i is the natural frequency of the i-order mode.

By combing Eqs. (11) and (12), the cross-covariance matrix $\left[C_{pp}\right]_r$ of $\{P_{eqq}\}_r$ can be expressed as

$$\begin{aligned}\left[C_{pp}\right]_r &= \overline{\{P_{eqq}\}_r\{P_{eqq}\}_r} = [M][\Phi][\Lambda]\overline{\{q(t)\}_r\{q(t)\}_r}[\Lambda]^T[\Phi]^T[M]^T \\ &= [M][\Phi][\Lambda]\left[C_{qq}\right]_r[\Lambda]^T[\Phi]^T[M]^T \\ &= [M][\Phi][\Lambda]\int_{-\infty}^{\infty}\dot{H}^*\Phi^T RDS_{AA}D^T R^T \Phi \dot{H}\, d\omega[\Lambda]^T[\Phi]^T[M]^T\end{aligned} \tag{13}$$

It is easy to find that $\{P_{eqq}\}_r$ is an elastic restoring force vector including resonance components only, and the precision mainly depends on the number of modal orders chosen for calculating $\{q(t)\}_r$ and the dynamic characteristics of the structure.

6.3 Resonant components and corresponding resonance equivalent static wind loads (ESWLs) based on the LRC method

According to the LRC method, the solving of resonant component and corresponding equivalent static wind loads can be translated into the solving of quasi-static response of the structure under the effect of $\{P_{eqq}\}_r$, which can be expressed as

$$\left\{r(t)\right\}_r = [I]\left\{P_{eqq}\right\}_r \tag{14}$$

The covariance matrix of resonant components is

$$\begin{aligned}\left[C_{rr}\right]_r &= \overline{\left\{r(t)\right\}_r\left\{r(t)\right\}_r} = [I]\left[C_{pp}\right]_r[I]^T = [I][M][\Phi][\Lambda]\left[C_{qq}\right]_r[\Lambda]^T[\Phi]^T[M]^T[I]^T \\ &= [I][M][\Phi][\Lambda]\int_{-\infty}^{\infty}\dot{H}^*\Phi^T RDS_{AA}D^T R^T\Phi\dot{H}\, d\omega[\Lambda]^T[\Phi]^T[M]^T[I]^T\end{aligned} \tag{15}$$

The resonance components of the structure is

$$\sigma_{R,r} = \sqrt{diag(\left[C_{rr}\right]_r)} \tag{16}$$

in which $diag(\bullet)$ is the column vector composed of the diagonal elements of the matrix.

The corresponding resonance equivalent static wind load $\boldsymbol{P}_{eBi}$ is

$$\boldsymbol{P}_{eBi} = \left[C_{pp}\right]_{\boldsymbol{r}}\boldsymbol{I}_i^T \big/ \sigma_{Ri,r} \tag{17}$$

in which $\boldsymbol{I}_i$ is row vector of the flexibility matrix I.

According to the ideas above, covariance matrix of total fluctuating response $\left[C_{rr}\right]_t$ can be obtained if the resonant transfer function $\overset{\bullet}{H}$ is replaced by transfer function H in Eq. (15).

The covariance matrix of background components based on the LRC method is

$$\left[C_{rr}\right]_b = [I]\left[C_{pp}\right][I]^T \tag{18}$$

in which $\left[C_{pp}\right]$ is the covariance matrix of external stochastic wind excitation.

The background components of the structure $\boldsymbol{\sigma}_{R,b}$ is

$$\sigma_{R,b} = \sqrt{diag([C_{rr}]_b)} \tag{21}$$

The covariance matrix of cross components considering the coupling effects between background and resonant components can be obtained based on the CCM method (Ke *et al*. 2012),

$$\left[C_{rr}\right]_c = \left[C_{rr}\right]_t - (\left[C_{rr}\right]_b + \left[C_{rr}\right]_r) \tag{20}$$

The cross components of the structure $\sigma_{R,c}$ is

$$\sigma_{R,c} = \sqrt{diag([C_{rr}]_c)} \tag{21}$$

The total fluctuating response $\boldsymbol{\sigma}_{R,t}$ can be expressed as

$$\sigma_{R,t} = \sqrt{\sigma_{R,b}^2 + \sigma_{R,r}^2 + sign([C_{rr}]_c)\sigma_{R,c}^2} \tag{22}$$

in which $sign(\bullet)$ is the sign function.

6.4 Numerical analysis for wind-induced effect of the 215 m cooling tower

In order to deeply research the contribution of three components (resonant component, background component and cross component) to the total fluctuating response, three components are calculated using the formula above based on the wind tunnel test of aero-elastic model of the 215m cooling tower. Fig. 9 shows the change curve of each component along the circular direction in the throat section (the section of outsec10 in Fig. 6(a)). It can be found that resonant components are dominated in the fluctuating wind-induced response of the cooling tower structure. The values of background components and cross components are in the same order of the magnitude which indicates that cross components cannot be ignored in relation to the high tower structure with a strong coupling flexibility, and shall be considered in the total fluctuating response combination.

The wind-induced response of the cooling tower is calculated by means of the CQC method of different orders, as well as the SRSS without considering the modal coupling effect method and the method proposed in the paper, and evaluated by taking the CQC calculation results of the full mode as standards. Fig. 10(a) shows the CQC calculation results of different orders for the circular section of the throat part of the tower. It can be found that with the increase of the order, the structural response value is gradually increased, specifically the response value is stable when the order is increased to 50, which is basically the same with the calculation results of full mode. It also indicates that the mode calculation results of the first order based on GLF and IWL methods are much lower than the value of the actual response. Figs. 10(b) and 10(c) show the calculation results of SRSS method and the method proposed in this paper and the calculation error to the CQC with full orders between them. It indicates that the impact of ignored modal coupling effects on cooling towers is large, and the coupling effects can be considered well by using the method proposed in the paper as the average error is about only 2% compared to that of SRSS method of 15%.

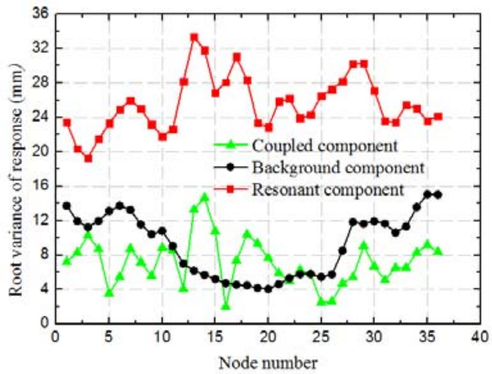

Fig. 9 Distribution chart of three components

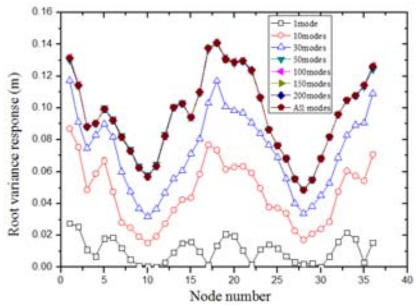

(a) CQC calculation results of different orders

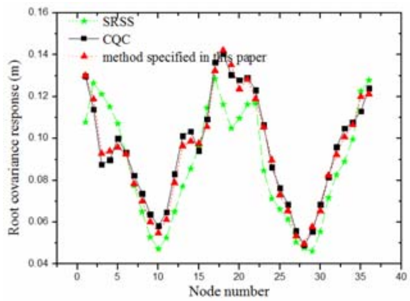

(b) Comparison of SRSS, method specified in the paper and full mode CQC calculation results

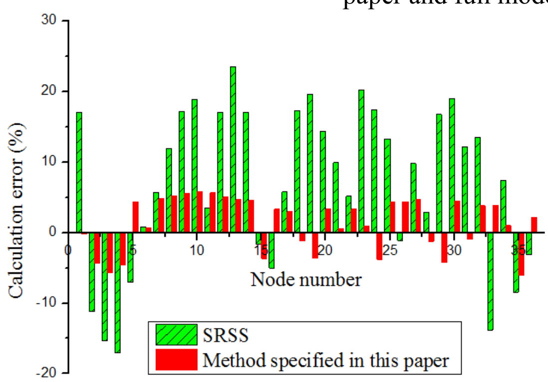

(c) Calculation error of SRSS and the method specified in the paper

Fig. 10 Comparisons of wind-induced displacement calculated with different methods

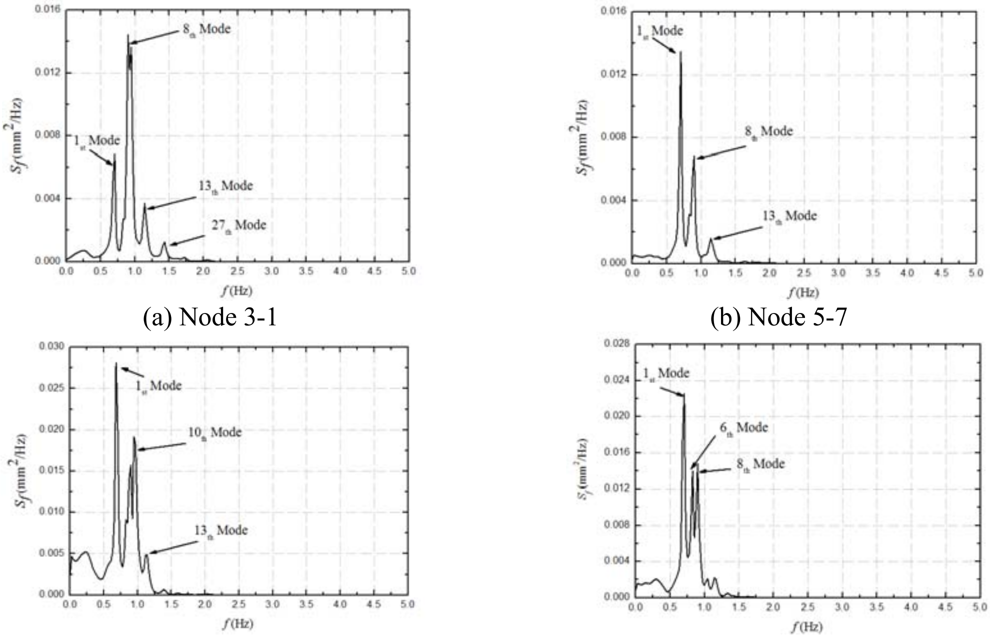

(a) Node 3-1 (b) Node 5-7

(c) Node 8-19 (d) Node 10-8

Fig. 11 Power spectrum density of displacement responses for typical nodes

Fig. 11 show the density function curves for the displacement fluctuating response power spectrum of the four nodes along the different circular angles of the different sections (Node a-b means the bth node along the circular direction of ath layer section in the Fig. 6(a)). It can be indicated that the wind-induced fluctuating response of super-large cooling towers are mainly excited by the resonant components and the mode for excitating the resonance components is different with the node in different regions. For example, the energy of Node 5-7 (see Fig. 11(b)) is mainly contributed by the resonant mode of 1-order and 8-order; but the energy contributed by the first order of the node 3-1 (see Fig. 11(a)) is relatively small and mainly contributed by the mode of 8-order. Therefore, it can be believed that the GLF method and IWL method only considering the mode effect of first order are not suitable for the wind-induced vibration response calculation of super-large cooling towers, so the resonance effect of multiple orders and the even high order mode must be considered in the wind-induced vibration analysis.

7. Conclusions

- In allusion to traditional continuous medium aero-elastic models of cooling towers which have some shortages in actual engineering application due to the characteristics of model design and processing, the "equivalent beam-net design method" of aero-elastic models of cooling towers is proposed. The formula of reduced-scale stiffness algorithm and corresponding modification and simulation methods about aerodynamic effects of Reynolds and Strouhal number are also given. The great advantage of the equivalent beam-net method is that the stiffness of the vertical and horizontal beam can be optionally regulated to solve the problem for the inconsistent scale ratio between the axial stiffness and the bending and torsion stiffness of the shell. Generally, the aero-elastic model designed by means of this method can obtain better results during the dynamic characteristics test process.

- This paper compares the distribution characteristics of the average surface wind pressure and root variance of fluctuating wind pressure based on the improved aero-elastic model while considering self-excited force effect. The biggest difference for the surface circumferential motion characteristics while considering self-excited force effect is that the minimum pressure coefficient angle is increased by 10°. The impact of self-excited force effect of large cooling towers on the average surface wind pressure is very small. The symmetry of the root variance distribution is completely broken and the numerical value of root variance is relatively large when the fluctuating wind pressure includes the self-excited force effect.
- According to the wind load and wind-induced performance obtained by means of wind tunnel test, the paper researches the wind-induced response characteristics of super-large cooling towers by means of the proposed method, showing that the background, resonant and cross components of such a flexible structure should not be ignored, especially the resonant components play a dominant role in the fluctuating response.
- By comparing the fluctuating response calculated by SRSS method and the method proposed in this paper with the calculation results of CQC method with full orders, it can be indicated that the method specified in the paper is featured with a relatively high accuracy and the calculation error using SRSS method is relatively large, so it can infer that the SRSS method used in actual engineering applications may have a potential safety hazard.
- From power spectrum density of displacement responses of some typical nodes, it can be found that the resonance effect of multiple orders and the even high order mode must be considered in the wind-induced vibration analysis of super-large cooling towers and the GLF method and IWL method only considering the mode effect of first order are not suitable for the wind-induced vibration response calculation.

Acknowledgements

The authors gratefully acknowledge the support of National Key Basic Research Program of China (i.e., 973 Program) (2013CB036300), Ministry of transport application foundation research project (2013319822070) and the National Natural Science Foundation of China (91215302, 51222809 and 51178353), and the support of Program for New Century Excellent Talents in University.

References

Armitt, J. (1980), “Wind loading on cooling towers”, *J. Struct. Div. - ASCE*, **106**(3), 623-641.

Babu, G.R., Rajan, S.S., Harikrishna, P., Lakshmanan, N. and Arunachalam, S. (2013), “Experimental determination of wind-induced response on a model of natural draught cooling tower”, *Exp. Techniques*, **37**(1), 35-46.

Bamu, P.C. and Zingoni, A. (2005), “Damage, deterioration and the long-term structural performance of cooling-tower shells: a survey of developments over the past 50 years’’, *Eng. Struct.*, **27**(12), 1794-1800.

Borri, C., Lupi, F. and Niemann, H.J. (2011), “Non-conventional wind loading on ultra-high towers in solar updraft power plants", *Proceedings of the 13th International Conference on Wind Engineering*, Netherlands, Amsterdam.

Davenport, A.G. (1967), "Gust loading factors", *J. Struct. Div. - ASCE*, **93**(3), 11-34.

DL/T 5339-2006. (2006), *Code for hydraulic design of fossil fuel power plants*, Development and Reform Commission, P.R.C.

GB/T 50102-2003. (2003), *Code for design of cooling for industrial recirculating water*, Ministry of Construction, P.R.C.

Goudarzi, M.A. and Sabbagh-Yazdi and S.R. (2008), "Modeling wind ribs effects for numerical simulation external pressure load on a cooling tower of KAZERUN power plant-IRAN", *Wind Struct.*, **11**(6), 479-496.

Isyumov, N., Abu-Sitta, S.H. and Davenport, A.G. (1972), "Approaches to the design of hyperbolic cooling towers against the dynamic action of wind and earthquakes", *Bull. Int. Assoc. Shell Struct.*, **48**, 35-47.

Kasperski, M. and Niemann, H.J. (1992), "The LRC (load-response correlation) method: a general method of estimating unfavorable wind load distributions for linear and nonlinear structural behavior", *J. Wind Eng. Ind. Aerod.*, **43**(1-3), 1753-1763.

Ke, S.T., Ge, Y.J., Zhao, L. and Tamura, Y. (2012), "A new methodology for analysis of equivalent static wind loads on supper-large cooling towers", *J. Wind Eng. Ind. Aerod.*, **111**, 30-39.

Li, F.H., Ni, Z.H., Shen, S.Z. and Gu, M. (2009), "Theory of POD and its application in wind engineering of structures", *J. Vib. Shock*, **28**(4), 29-32 (in Chinese).

Meroney, R.N. (2008), "Protocol for CFD prediction of cooling-tower drift in an urban environment", *J. Wind Eng. Ind. Aerod.*, **96**(10), 1789-1804.

Murali, G., Vardhan, C.M.V. and Reddy, B.V.P (2012), "Response of cooling towers to wind loads", *J. Eng. Appl. Sci.*, **7**(1), 114-120.

Niemann, H.J. and Köpper, H.D. (1998), "Influence of adjacent buildings on wind effects on cooling towers", *Eng. Struct*., **20**(10), 874-880.

Orlando, M. (2001), "Wind-induced interference effects on two adjacent cooling towers", *Eng. Struct.*, **23**, 979-992.

Simiu, E. and Scanlan, R.H. (1996), *Wind effects on structures: fundamentals and applications to design*, John Wiley & Sons, Inc. Chapter 11: Hyperbolic cooling towers, 404-419, New York.

Tamura, Y. and Suganuma, S. (1999), "Proper orthogonal decomposition of random wind pressure field", *J. Fluid. Struct.*, **13**(7-8), 1069-1095.

Xu, Y.Z. and Bai G.L. (2013), "Random buckling bearing capacity of super-large cooling towers considering stochastic material and wind loads", *Probabilist. Eng. Mech.*, **33**, 18-25.

Zahlten, W. and Borri, C. (1998), "Time-domain simulation of the non-linear response of cooling tower shells subjected to stochastic wind loading", *Eng. Struct.*, **20**(10), 881-889.

Zhang, X.T. (2002), "Evaluation and prospect for wind loading codes at home and abroad", *J. Tongji University*, **30**(5), 539-543 (in Chinese).

Zhao, L., Lu, A.P., Zhu, L.D., Cao, S.Y. and Ge, Y.J. (2013), "Radial pressure profile of typhoon field near ground surface observed by distributed meteorologic stations", *J. Wind Eng. Ind. Aerod.*, **122**, 105-112.

Zhao, L. and Ge, Y.J. (2010), "Wind loading characteristics of super-large cooling towers", *Wind Struct*., **13**(4), 257-274.

CC